[6]Davison, E. J., and Ramesh, N., "A Note on the Eigenvalues of a Real Matrix," *IEEE Transactions on Automatic Control*, Vol. AC-15, No. 2, 1970, pp. 252, 253.

Nonlinear Dynamics of the Tethered Subsatellite System in the Station Keeping Phase

Hironori A. Fujii* and Wakano Ichiki†
Tokyo Metropolitan Institute of Technology, Hino, Tokyo 191, Japan

I. Introduction

THE tethered subsatellite system[1–5] (TSS) mission requires three phases: deployment, station keeping, and retrieval. Let us focus on the analysis of the nonlinear dynamics for the TSS in the station keeping phase, where tether is assumed to have constant natural length. Even in the station keeping phase, TSS motion shows highly nonlinear behavior taking into account complex effects caused by such perturbation parameters as the orbit eccentricity and the tether elasticity. Nonlinear dynamics is investigated in the literature[6–11] because the dynamics is not easily analyzed and exhibits interesting behavior such as chaos. Nonlinear analysis tools are employed in this study, such as Poincaré maps, bifurcation diagrams, and Lyapunov exponents, and show periodic, quasiperiodic, and chaotic motion, depending on each system parameter. Kanasopoulos and Richardson[6,7] investigated the nonlinear dynamics of a gravity-gradient satellite, and Nixon and Misra[8] did so for the TSS with a rigid tether. Our objective is not just an application of the nonlinear analysis but to point out the importance of the nonlinear analysis of TSS by taking into account the complex effects of its system parameters.

II. Equations of Motion

The TSS model treated in this paper is a gravity-gradient tethered subsatellite in an elliptical orbit. Eccentricity and the longitudinal rigidity of tether are chosen for the system parameters. Energy dissipation such as the aerodynamic effect will be ignored in this system. The dynamical model is simplified by employing the following assumptions.

1) The Shuttle and subsatellite are point masses.

2) The center of mass of the system coincides with that of the Shuttle.

3) Tether length is sufficiently smaller than the distance between the Shuttle and the center of the Earth.

4) The tether is approximately regarded as a linear spring whose natural length is 100 km, and its mass is negligible.

The equations of motion for TSS for two cases are described as follows.

1) The first case is that of a circular orbit, and the tether has no elasticity:

$$\ddot{\theta} = -\tfrac{3}{2}\sin(2\theta) \tag{1}$$

2) The second case is that of an elliptical orbit,[12] and the tether has elasticity[4] in the pitch rotation direction,

$$l(1+e\cos\eta)\ddot{\theta} - 2el(\dot{\theta}+1)\sin\eta + \tfrac{3}{2}l\sin 2\theta + 2(1+e\cos\eta)(\dot{\theta}+1)\dot{l} = 0 \tag{2}$$

and in the tether length direction,

$$(1+e\cos\eta)\ddot{l} - 2e\sin\eta\,\dot{l} - l(1+e\cos\eta)(2+\dot{\theta})\dot{\theta} - 3l(1+e\cos\eta)\cos^2\theta + (T/m)(R^3/\mu) = 0 \tag{3}$$

l, θ, l_0, m, a, e, μ, and EA denote tether length, pitch rotation, natural length of tether, mass of subsatellite, semimajor radius (which is constant at 6600 km in this case), eccentricity of orbit, gravitational constant, and the longitudinal rigidity of tether, respectively. The tension of the tether T and the orbit radius R are defined as $T = EA(l - l_0)/l_0$ and $R = a(1-e^2)/(1+e\cos\eta)$, respectively, where η denotes true anomaly and indicates the independent variable.

III. Chaos

Chaos is introduced here to recognize the employed nonlinear analysis. Chaotic motion means that the behavior of the system can be predicted for the short term but cannot for all of the time, and the motion is regarded as chaotic if it simultaneously satisfies the following two properties[11]: sensitive dependence on the initial conditions and topological transition. When the equations of motion are nonlinear and do not have analytical solutions, the motion becomes chaotic over some range of the initial conditions or system parameters. Concerning TSS, two system parameters, eccentricity and the longitudinal rigidity of tether, can affect the nonlinear dynamics through the coefficients of nonlinear terms. Therefore, chaotic motion may occur in the situation by taking either of them into account, as in Eqs. (2) and (3). On the other hand, chaotic motion never occurs in the situation without taking both of them into account, as in Eq. (1).

IV. Poincaré Maps

A Poincaré map is a collection of discrete plots created by integrating the equations of motion and periodically sampling the following particular points in the trajectory[6,7,10]:

$$\theta_n = \theta(\eta_n) \tag{4}$$

$$\dot{\theta}_n = \dot{\theta}(\eta_n) \tag{5}$$

where $\eta_n = \eta_0 + n\Delta\eta$ ($n = 0, 1, 2, \ldots, N$) and n is the number of orbits. Here, Poincaré maps are drawn by gathering these points until $N = 100$ once per orbit, where the subsatellite passes through perigee with many initial conditions. On the Poincaré map, periodic motion is shown as one or more fixed points, quasiperiodic motion as a closed curve if a sufficient number of points are plotted, and chaotic motion as a scattering of points.

A Poincaré map in the rigid-body tether system with constant eccentricity, $e = 0.0$, is shown in Fig. 1. The origin and $(\theta, \dot{\theta}) = (\pm\pi, 0)$ are stable equilibriums, and $(\theta, \dot{\theta}) = (\pm\pi/2, 0)$ are unstable equilibriums. In the stable equilibriums, the motion of the TSS has one period in a synchronous orbit and the tether directs toward the local vertical direction. In the unstable equilibriums, at a distance $\pi/2$ rad from stable equilibriums, the tether directs along the local horizontal. The TSS motion is separated into two parts by a separatrix passing through unstable equilibriums, that is, the motion is libration inside the separatrix and tumbling outside the separatrix. Perturbing at eccentricity, $e = 0.05$ as in Fig. 2, chaos occurs in the neighborhood of the unstable equilibriums.

V. Bifurcation Diagrams

A bifurcation diagram is constituted by sampling points of $\theta(\eta_n)$ in the trajectory, corresponding with Eq. (4) in the same way as for the Poincaré maps, and is plotted with respect to eccentricity for a stable equilibrium point.

Bifurcation diagrams are shown in Figs. 3 and 4 for the case of the rigid-body tether system and the elastic tether system for $EA = 10^4$ N, respectively. These diagrams clarify the process that a stable equilibrium, whose period is one per one orbit at the initial state, bifurcates to different equilibriums whose periods are not one per one orbit. The motion of period 3 appears at $e = 0.25$ and 0.20,

Received July 22, 1996; revision received Nov. 26, 1996; accepted for publication Dec. 2, 1996.

*Professor, Department of Aerospace Engineering. Associate Fellow AIAA.

†Graduate Student, Department of Aerospace Engineering.

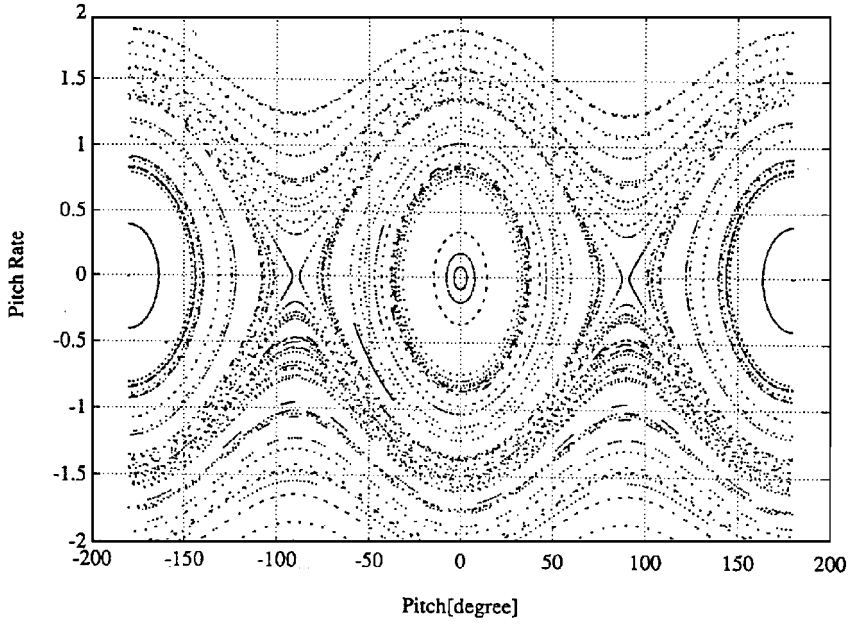

Fig. 1 Poincaré map for $e = 0.0$.

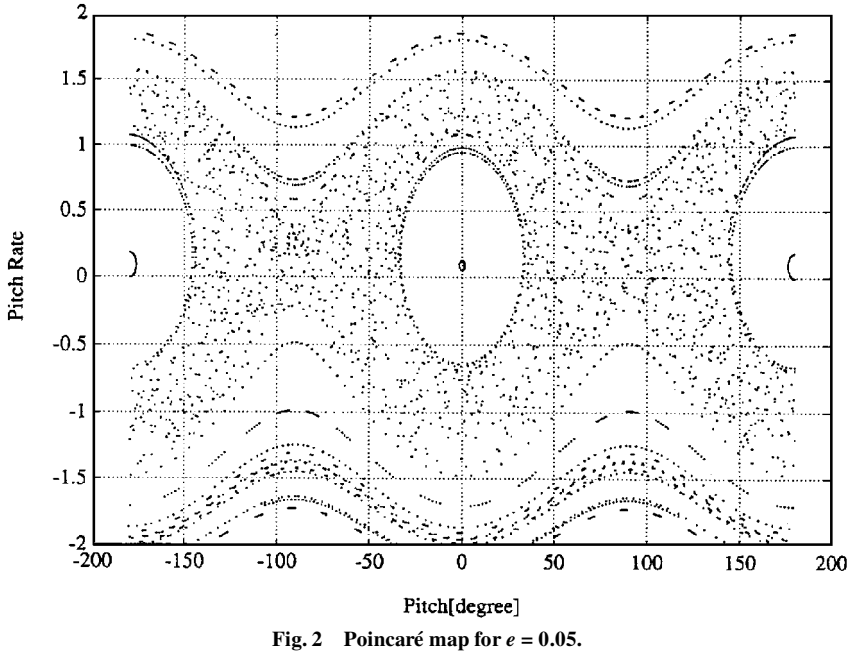

Fig. 2 Poincaré map for $e = 0.05$.

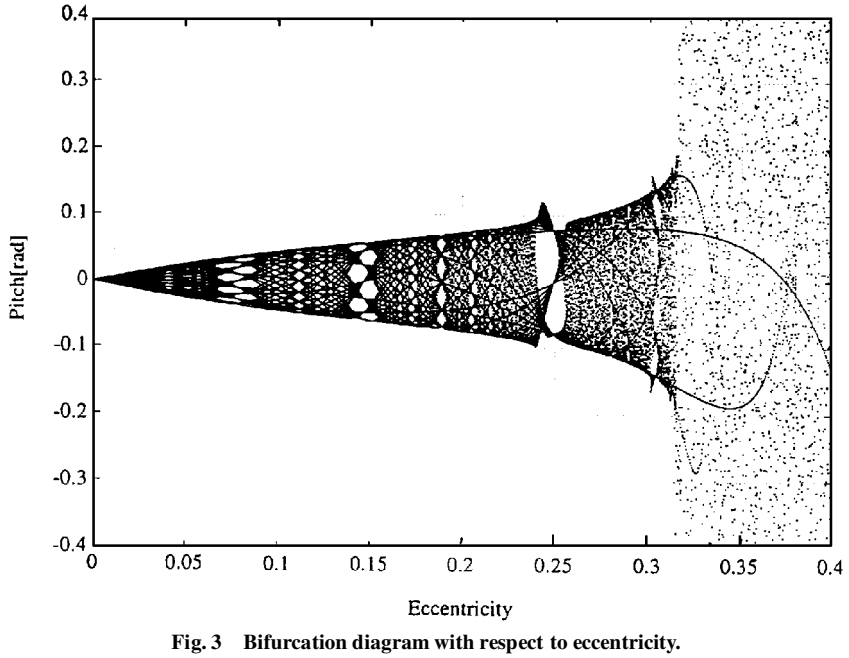

Fig. 3 Bifurcation diagram with respect to eccentricity.

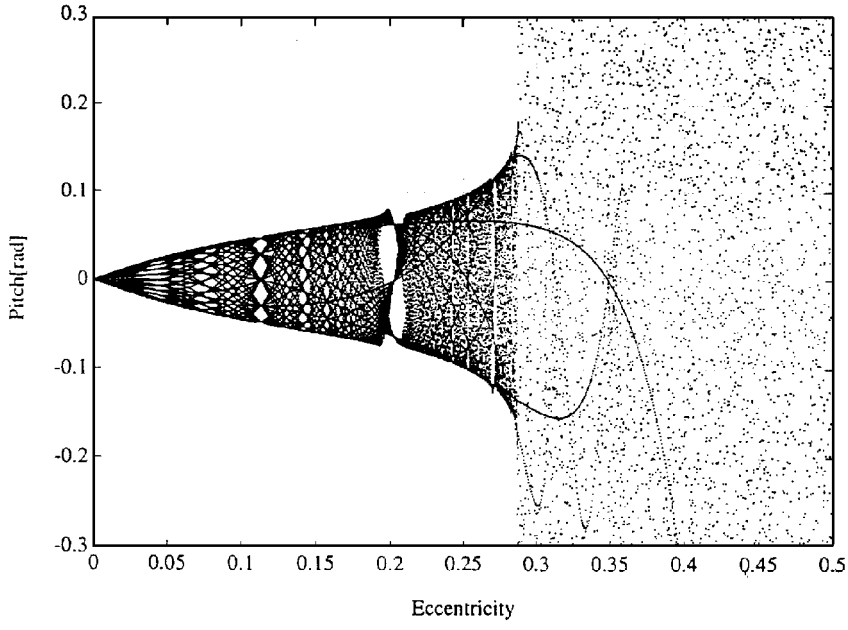

Fig. 4 Bifurcation diagram with respect to eccentricity at $EA = 10^4$ N.

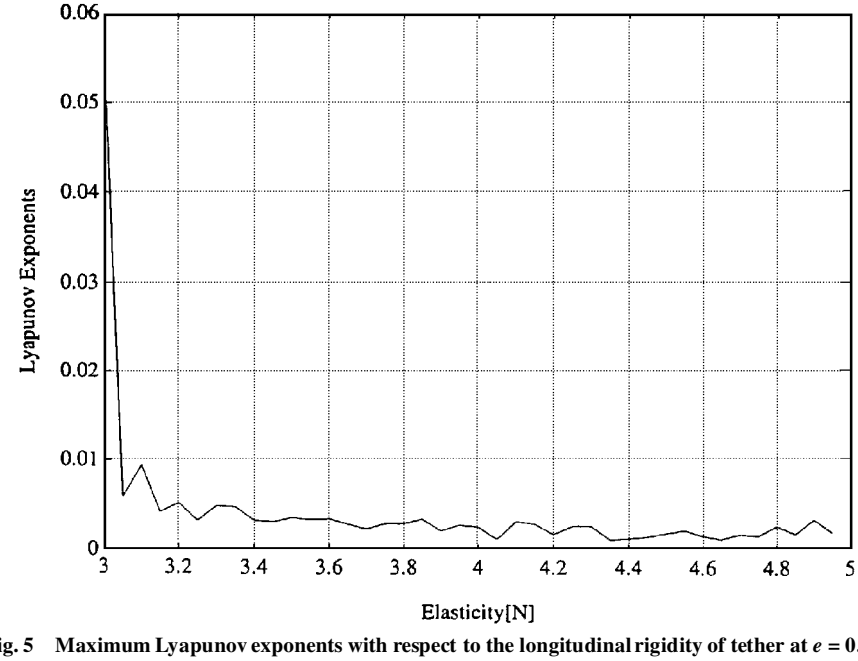

Fig. 5 Maximum Lyapunov exponents with respect to the longitudinal rigidity of tether at $e = 0.01$.

and chaotic motion appears at $e > 0.31$ and 0.28, as shown in Figs. 3 and 4, respectively.

VI. Lyapunov Exponents

Lyapunov exponents indicate the average of exponential divergence or convergence of the nearby orbits in the n-dimensional phase space. Hence, $P_i(0)$ denotes the ith radius of the n sphere for the initial state and $P_i(t)$ is the radius of the n ellipsoid deformed by nature of the flow after a long-term evolution. The ith Lyapunov exponents are defined as follows[9]:

$$\lambda_i = \lim_{t\to\infty} (1/t) \log_2[P_i(t)/P_i(0)] \tag{6}$$

where λ_i is ordered from largest to smallest in its value.

It is evident from Eq. (6) that $\lambda_i = 0$ for $P_i(0) = P_i(t)$, $\lambda_i < 0$ for $P_i(0) > P_i(t)$, and $\lambda_i > 0$ for $P_i(0) < P_i(t)$, which lead to the observation that Lyapunov exponents equal to or less than zero result in regular motion and those larger than zero result in chaotic motion. As the positive maximum Lyapunov exponents increase, the motion becomes more chaotic. A stable equilibrium point is chosen for the initial condition.

A variation of the maximum Lyapunov exponents is shown in Fig. 5 with constant eccentricity at $e = 0.01$ with respect to the variation of the longitudinal rigidity of the tether. The maximum Lyapunov exponents decrease as the longitudinal rigidity of the tether increases; that is, the motion becomes more periodic in proportion to the increase of the longitudinal rigidity of the tether. The maximum Lyapunov exponents suddenly decrease at $EA = 10^{3.05}$ N, which is the border where the motion becomes less chaotic.

A variation of the maximum Lyapunov exponents is shown in Fig. 6 with the constant longitudinal rigidity of the tether at $EA = 10^4$ N with respect to the variation of the eccentricity. The motion generally becomes more chaotic in proportion to the increase of the eccentricity, and the maximum Lyapunov exponents suddenly increase at $e = 0.27$.

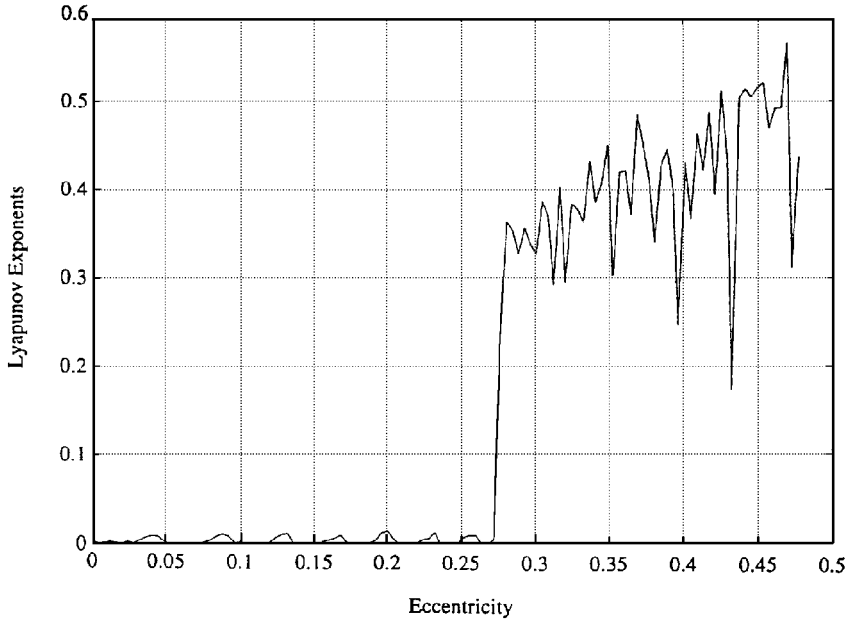

Fig. 6 Maximum Lyapunov exponents with respect to eccentricity at $EA = 10^4$ N.

VII. Conclusion

The nonlinear dynamics of the TSS with constant natural length of tether is analyzed by taking into account the complex effects of two system parameters, the orbital eccentricity of the Shuttle and the longitudinal rigidity of the tether. Taking one of them into account for consideration, the motion of TSS becomes chaotic depending on the system parameters and the initial conditions.

Poincaré maps, bifurcation diagrams, and Lyapunov exponents are used to analyze the nonlinear dynamics of the TSS. Poincaré maps show the global motion of the system for many initial conditions. We have focused especially on the dynamics around the stable equilibrium point by using two other nonlinear analysis tools, bifurcation diagrams and Lyapunov exponents: the first shows the process of transition from regular to chaotic motion perturbed at eccentricity, and the second reveals the chaotic degree perturbed at each of the system parameters.

Emergence of the chaotic motion can be avoided by selecting eccentricity and the longitudinal rigidity of the tether based on the results of the present study, and these analytical results would be useful for the operational mission of the TSS.

References

[1]Rupp, C. C., and Laue, J. H., "Shuttle/Tethered Subsatellite System," *Journal of the Astronautical Sciences*, Vol. 26, No. 1, 1978, pp. 1–17.

[2]Misra, A. K., and Modi, V. J., "A Survey on the Dynamics and Control of Tethered Satellite Systems," *Tethers in Space, Advances in the Astronautical Sciences*, Vol. 62, American Astronautical Society, San Diego, CA, 1987, pp. 667–719.

[3]Bekey, I., "Tether Open New Space Options," *Astronautics and Aeronautics*, Vol. 21, No. 4, 1983, pp. 32–40.

[4]Onoda, J., and Watanabe, N., "Tethered Subsatellite Swinging from Atmospheric Gradients," *Journal of Guidance, Control, and Dynamics*, Vol. 11, No. 5, 1988, pp. 477–479.

[5]Kokubun, K., Fujii, H. A., and Oyama, K., "Effect of Aerodynamic Force on the Japanese Tethered Satellites," *Proceedings of the 39th Space Sciences and Technology Conference*, Vol. 31, Japan Society for Aeronautical and Space Sciences, Osaka, Japan, 1995, pp. 107, 108 (in Japanese).

[6]Kanasopoulos, H. A., and Richardson, D. L., "Chaos in the Pitch Equation of Motion for the Gravity-Gradient Satellite," AIAA Paper 92-4369, Aug. 1992.

[7]Kanasopoulos, H. A., and Richardson, D. L., "Numerical Investigation of Chaos in the Attitude Motion of a Gravity-Gradient Satellite," AAS/AIAA Astrodynamics Specialist Conf., AAS-93-581, Victoria, BC, Canada, Aug. 1993.

[8]Nixon, M. S., and Misra, A. K., "Nonlinear Dynamics and Chaos of Two-Body Tethered Satellite Systems," AAS/AIAA Astrodynamics Specialist Conf., AAS-93-731, Victoria, BC, Canada, Aug. 1993.

[9]Wolf, A., Swift, J. B., Swinny, H. L., and Vastano, J. A., "Determining Lyapunov Exponents from a Time Series," *Physica 16D*, North-Holland, Amsterdam, 1985, pp. 285–317.

[10]Parker, T. S., and Chua, L. O., "Chaos: A Tutorial for Engineers," *Proceedings of the IEEE*, Vol. 75, No. 8, 1987, pp. 982–1008.

[11]Wiggins, S., *Introduction to Applied Nonlinear Dynamics System and Chaos*, Springer-Verlag, New York, 1990, Chap. 4.

[12]Hughes, P. C., *Spacecraft Attitude Dynamics*, Wiley, New York, 1986, pp. 308–313.